Oligothiophene-Based Photovoltaic Materials for Organic Solar Cells: Rise, Plateau, and Revival

Tainan Duan[a,+,*], Qianqian Chen[a,+], Dingqin Hu[a], Jie Lv[a], Donghong Yu[b,c], Gang Li[d,*], and Shirong Lu[a,*]

[a] Chongqing Institute of Green and Intelligent Technology, Chongqing School, University of Chinese Academy of Sciences (UCAS Chongqing)
Chinese Academy of Sciences, Chongqing, 400714, China.
E-mail: tnduan@cigit.ac.cn, lushirong@cigit.ac.cn.

[b] Department of Chemistry and Bioscience, Aalborg University, Aalborg, DK 9220, Denmark.

[c] Sino-Danish Center for Education and Research, Aarhus, DK 8000, Denmark.

[d] Department of Electronic and Information Engineering, Research Institute for Smart Energy (RISE), The Hong Kong Polytechnic University, Hung Hom, Kowloon, Hong Kong, P. R. China

E-mail: gang.w.li@polyu.edu.hk

[+] These authors contributed equally to this work.

Abstract

Oligothiophene derivatives, with superior charge transport, excellent intrinsic stability, and low synthetic cost, have been positioned as one of the most promising donor materials in cost-effectiveness and large-scale production. From the 1990s to date, oligothiophene donors have been popularized in the *era* of fullerene acceptors but suffered repeated failures in the new *era* of nonfullerene acceptors (NFAs). Recently, organic solar cells (OSCs) fabricated with oligothiophene donors achieved a power conversion efficiency of 15.4%, which enabled researchers to refocus on these old yet blooming materials. Herein, the development of oligothiophene-based photovoltaic materials and their applications in OSCs are chronologically presented. The evolution of molecular design in oligothiophene donors and certain milestone materials are highlighted and emphasized. Recently published inspiring

results on oligothiophene-based NFAs are included. To offer guidance for researchers and spur further development of oligothiophene-based photovoltaic materials, we propose a perspective on future trends in the molecular design and applications of oligothiophene donors/acceptors.

Organic Solar Cells: From Polymers to Small Molecules

Through the efficient direct conversion of solar irradiation to electricity, solar cells have become one of the most important solutions to the energy demand.[1,2] Distinct from its inorganic predecessors (silicon- , GaAs- and CuInGaSe-based solar cells), organic solar cells (OSCs) exhibit unique advantages, such as environmental friendliness, solution processability, and flexibility.[3-7]

Considering the bulk heterojunction (BHJ) architecture as the cornerstone (**BOX 1**), OSC-related studies have received exponentially increased attention and achieved continuously enhanced PCE values in the following two decades along with the emergence of uncountable new organic photovoltaic materials, as well as interface and device engineering. [13-19] In particular, recently, the rise of small molecule (SM) nonfullerene acceptors (NFA) improved the PCEs of OSCs.[20-26] By employing state-of-the-art polymer donor/NFA binaries, PCEs over 18% have been achieved in single-junction OSCs.[27-29] However, considering that the mass production of photovoltaic materials is necessary for the commercialization of OSCs, the inconsistent device performance caused by the batch-to-batch variations in molecular weight (M_w) and polydispersity index (M_w/M_n) of polymers remains a major challenge.[30-33] Therefore, researchers have turned to SM donors, which exhibit excellent batch-to-batch invariability in photovoltaic behavior and well-defined easily tunable structure.[34,35]

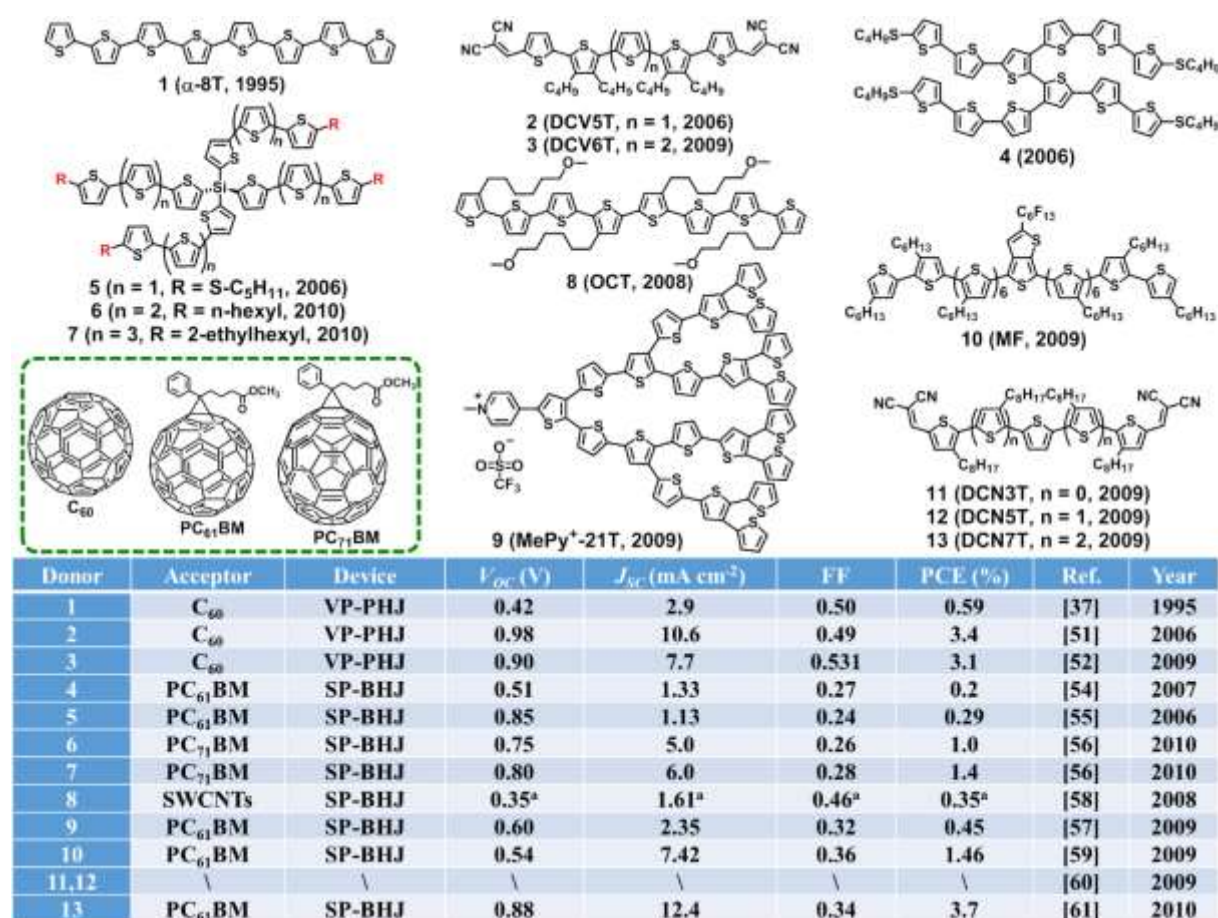## Oligothiophene Based Small Molecule Materials
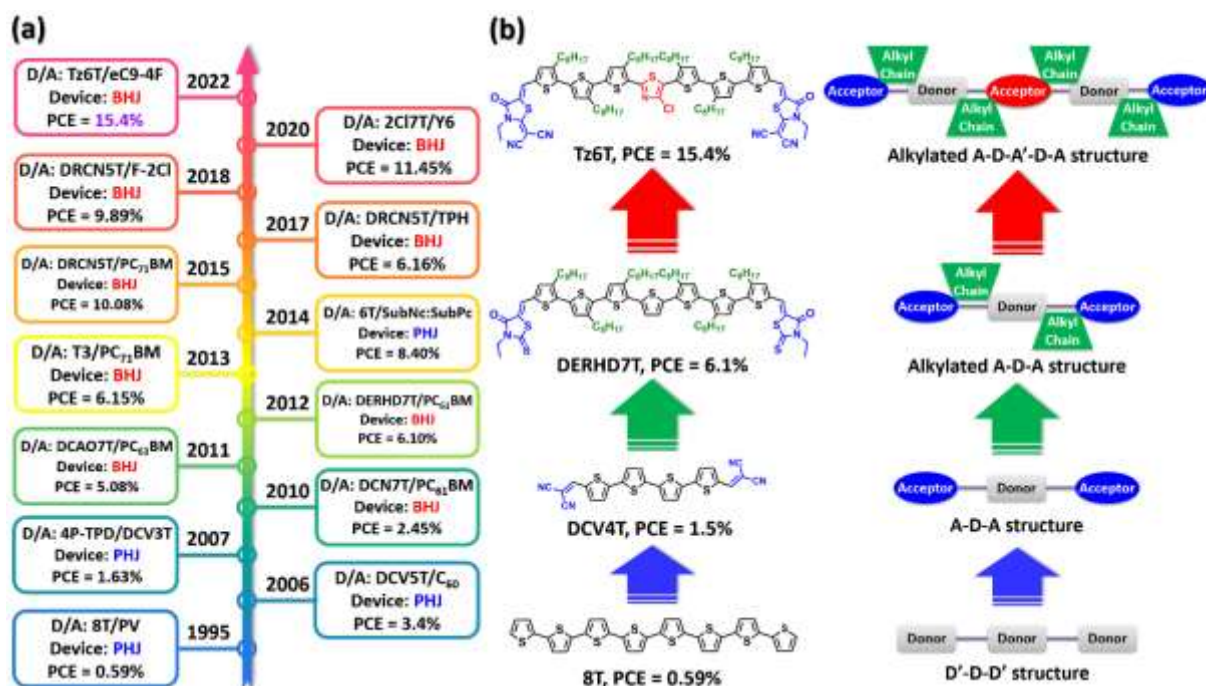
Figure 1. a) A brief timeline on the development of oligothiophene-based photovoltaic materials. b) The structural evolution of oligothiophene donors.

Oligothiophenes, an old but thriving family of conjugated materials, are widely used as an active component in organic electronic devices, such as light-emitting diodes (OLEDs), field-effect transistors (OFETs), and OSCs.[36] α-octithiophene (8T, **Figure 1b**) was first adopted as an electron donor in OSCs in 1995, and oligothiophenes have been intensively investigated as photoactive materials in OSCs since.[37,38] This is majorly because of their intriguing optoelectronic properties, charge-transporting properties, excellent intrinsic stability, and unique self-assembling properties on solid surfaces or in the bulk. Another key factor facilitating this development is that its well-established and enormously developed heterocyclic chemistry offers countless methods to modify the thiophene ring and generate kaleidoscopic π-conjugated systems at a high yield and low cost.[39-42] Owing to the unremitting efforts of researchers, oligothiophene-based photovoltaic compounds have evolved from pure thiophene oligomers to delicately constructed solution-processable

molecules (**Figure 1b**). Consequently, the PCE of oligothiophene-based OSCs was boosted from below 1% to over 15% (**Figure 1a**).

To ensure that this cost-effective donor family qualifies for the real production of commercialized OSCs in the future, further enhancement of the performance of oligothiophene donors is necessary. When designing a high-performance donor, a delicate control of multiple factors including energy levels, bandgap, solubility, crystallinity, and compatibility with acceptors is mandatory.[43] Therefore, a comprehensive retrospect on oligothiophene-based photovoltaic materials (**Box 2**) is urgently needed to endow researchers with inspiration by reviewing those old molecules.

Emergence and development: 1995–2010

Donor	Acceptor	Device	V_{OC} (V)	J_{SC} (mA cm^{-2})	FF	PCE (%)	Ref.	Year
1	C$_{60}$	VP-PHJ	0.42	2.9	0.50	0.59	[37]	1995
2	C$_{60}$	VP-PHJ	0.98	10.6	0.49	3.4	[51]	2006
3	C$_{60}$	VP-PHJ	0.90	7.7	0.531	3.1	[52]	2009
4	PC$_{61}$BM	SP-BHJ	0.51	1.33	0.27	0.2	[54]	2007
5	PC$_{61}$BM	SP-BHJ	0.85	1.13	0.24	0.29	[55]	2006
6	PC$_{71}$BM	SP-BHJ	0.75	5.0	0.26	1.0	[56]	2010
7	PC$_{71}$BM	SP-BHJ	0.80	6.0	0.28	1.4	[56]	2010
8	SWCNTs	SP-BHJ	0.35[a]	1.61[a]	0.46[a]	0.35[a]	[58]	2008
9	PC$_{61}$BM	SP-BHJ	0.60	2.35	0.32	0.45	[57]	2009
10	PC$_{61}$BM	SP-BHJ	0.54	7.42	0.36	1.46	[59]	2009
11,12	\	\	\	\	\	\	[60]	2009
13	PC$_{61}$BM	SP-BHJ	0.88	12.4	0.34	3.7	[61]	2010

Figure 2. Representative oligothiophenes reported during 1995–2010 along with the device parameters and fullerene-based acceptors mentioned in this paper (circled with a green dashed line).

The debut of oligothiophenes occurred in 1995. A simple structured α-octithiophene 8T (**1**) was employed as an electron donor to construct a vacuum-processed (VP) PHJ OSC with an electron-accepting perylene pigment PV.[37] Although only a modest PCE of *ca.* 0.6% was achieved, this study initiated the development of oligothiophene-based photovoltaic materials. However, owing to the considerably high PCEs of polymer donors (poly(3-hexylthiophene-2,5-diyl); P3HT),[50] oligothiophenes did not attract sufficient attention until a new century.

In 2006, Bäuerle *et al.* reported an oligothiophene derivative, DCV5T (**2**), structured with a pentathiophene backbone and two electron-withdrawing dicyanovinyl (DCV) terminal groups.[51] The DCV5T:C$_{60}$-based VP PHJ OSCs exhibited a high V_{OC} of 0.98 V with a J_{SC} of 10.6 mA cm^{-2} and a PCE of 3.4%, which was comparable to those of polymer donor-based devices. Based on DCV5T, DCV6T (**3**) was developed afterward but because of its decreased V_{OC} of 0.90 V, an inferior PCE of *ca.* 3.1% was observed.[52] Judging from the molecular structure, the introduction of DCV substituents with low-lying lowest unoccupied molecular orbital (LUMO) energy levels considerably reduced the corresponding optical gap, compared with that of the unsubstituted oligothiophene. Moreover, the terminal groups of the molecules were prone to be coupled with the neighboring thiophene cores in the solid state *via* intermolecular CN···H bonds.[53] This molecular arrangement might favor an attractive interaction between the transition dipoles of the intramolecular D–A excitations, thereby resulting in a red-shift in the absorption of thin films, compared with that of the molecules in solution. The broadened absorption would indisputably benefit the light-harvesting and subsequently enhance the J_{SC} of OSC devices. This A–π–D–π–A strategy greatly impacted

subsequent research; the electron-withdrawing terminal groups gradually became an indispensable part of high-performance SM photovoltaic molecules.

Attracted by the superiority of BHJ architecture and the convenience of the solution-processing technique, researchers began to focus on highly soluble oligothiophene donors to extend the boundary of materials development and break the limitations of the costly vacuum deposition technique. To alleviate the π–π stacking interaction and enhance the solubility of oligothiophenes, Roncali *et al.* synthesized "X-shaped" oligothiophene **4** in 2006. The solution processed (SP) BHJ OSCs based on **4**:$PC_{61}BM$ exhibited a PCE of *ca.* 0.2%; the fill factor (*FF)* of 0.27 and low J_{SC} of 1.33 mA cm^{-2} caused by the narrow absorption range of donor **4** drastically limited the device performance.[54] Similarly, a series of *tetrakis* oligothienylsilanes were developed. Compound **5** exhibited a modest PCE of *ca.* 0.29% because of the poor *FF* of 0.24. In other studies, the PCE was pushed to over 1.0% by modified molecules **6** and **7** with an extended π-conjugation and absorption range.[55,56] Certain dendritic oligothiophenes were designed and tentatively employed as donor materials. In 2009, Bäuerle *et al.* reported a branched oligothiophene salt, MePy$^+$-21T (**9**), bearing a methylpyridinium terminal group. Considering that the V_{OC} of **9**:$PC_{61}BM$-based BHJ OSCs was merely 0.6 V because of the high-lying highest occupied molecular orbital (HOMO) energy level of **9**, the PCE was below 1%.[57]
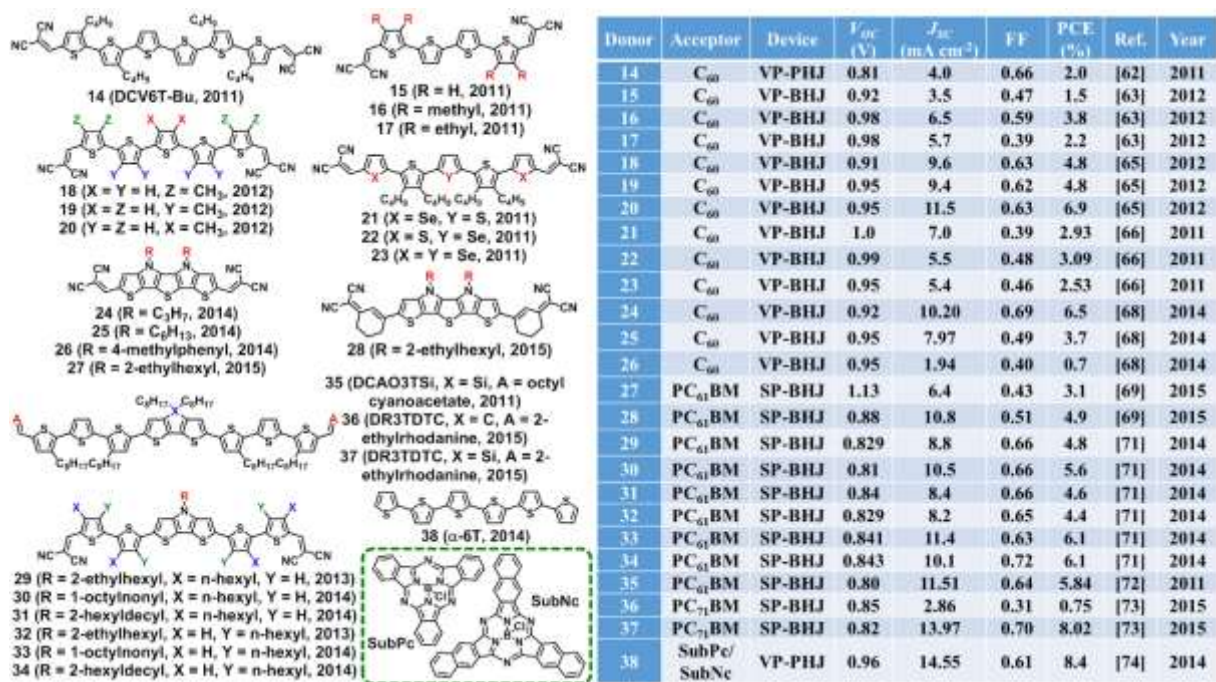
Another approach to soluble oligothiophenes is alkylation. Dissimilar to the construction of a three-dimensional (3D) or twisted structure, the attachment of flexible alkyl chains can enhance the solubility of molecules without sacrificing the planarity of the conjugated backbone or the intermolecular charge transfer from the electron-donating center to electron-withdrawing terminals. In 2008, Lanzi *et al.* synthesized an alkylated octithiophene, OCT (**8**); BHJ OSCs based on OCT films mixed with single-walled carbon nanotubes (SWCNTs, as acceptors) were prepared, and a PCE of 0.35% was realized.[58] Yu

et al. synthesized an oligomer, **MF**, containing 16 regioregular conjugated thiophene rings and an electron-withdrawing thieno[3,4-b]thiophene center (**10**).[59] Molecule **10** exhibited wide-range light-harvesting with an absorption onset of film approaching 800 nm and a fairly good PCE of 1.46%. This shed light on the pivotal role of regioregular π-linkers in oligothiophene donors. In 2009, Chen *et al.* reported a series of oligothiophene donors, DCN3T (**11**), DCN5T (**12**), and DCN7T (**13**). The suitable energy levels and conjugation length of DCN7T (**13**) resulted in a well-balanced V_{OC} of 0.88 V and J_{SC} of 12.4 mA cm^{-2}. A PCE of 3.7% was achieved using **13**:PC$_{61}$BM blends[60,61], which was among the best PCEs obtained for SP SM BHJ devices. DCN7T is historically recognized as one of the most important SM donor molecules. Its regioregular and axisymmetric A–π–D–π–A structure provides an excellent template for researchers and guided them toward efficient oligothiophene donors.

In this period, it was observed that solution processing was gradually replacing vacuum deposition in device fabrication. For materials development, owing to the limited papers and designs for reference, most studies on oligothiophene donors were not inherited. They were based on the exploration of new structures, investigating their impact on the performance of OSC devices and using the feedback to improvise. As a Chinese proverb says, "cross the river by feeling the stones." Fortunately, the right path was getting clearer.

Rise: 2011–2015

Donor	Acceptor	Device	V_{OC} (V)	J_{SC} (mA cm^{-2})	FF	PCE (%)	Ref.	Year
14	C$_{60}$	VP-PHJ	0.81	4.0	0.66	2.0	[62]	2011
15	C$_{60}$	VP-BHJ	0.92	3.5	0.47	1.5	[63]	2012
16	C$_{60}$	VP-BHJ	0.98	6.5	0.59	3.8	[63]	2012
17	C$_{60}$	VP-BHJ	0.98	5.7	0.39	2.2	[63]	2012
18	C$_{60}$	VP-BHJ	0.91	9.6	0.63	4.8	[65]	2012
19	C$_{60}$	VP-BHJ	0.95	9.4	0.62	4.8	[65]	2012
20	C$_{60}$	VP-BHJ	0.95	11.5	0.63	6.9	[65]	2012
21	C$_{60}$	VP-BHJ	1.0	7.0	0.39	2.93	[66]	2011
22	C$_{60}$	VP-BHJ	0.99	5.5	0.48	3.09	[66]	2011
23	C$_{60}$	VP-BHJ	0.95	5.4	0.46	2.53	[66]	2011
24	C$_{60}$	VP-BHJ	0.92	10.20	0.69	6.5	[68]	2014
25	C$_{60}$	VP-BHJ	0.95	7.97	0.49	3.7	[68]	2014
26	C$_{60}$	VP-BHJ	0.95	1.94	0.40	0.7	[68]	2014
27	PC$_{61}$BM	SP-BHJ	1.13	6.4	0.43	3.1	[69]	2015
28	PC$_{61}$BM	SP-BHJ	0.88	10.8	0.51	4.9	[69]	2015
29	PC$_{61}$BM	SP-BHJ	0.829	8.8	0.66	4.8	[71]	2014
30	PC$_{61}$BM	SP-BHJ	0.81	10.5	0.66	5.6	[71]	2014
31	PC$_{61}$BM	SP-BHJ	0.84	8.4	0.66	4.6	[71]	2014
32	PC$_{61}$BM	SP-BHJ	0.829	8.2	0.65	4.4	[71]	2014
33	PC$_{61}$BM	SP-BHJ	0.841	11.4	0.63	6.1	[71]	2014
34	PC$_{61}$BM	SP-BHJ	0.843	10.1	0.72	6.1	[71]	2014
35	PC$_{61}$BM	SP-BHJ	0.80	11.51	0.64	5.84	[72]	2011
36	PC$_{71}$BM	SP-BHJ	0.85	2.86	0.31	0.75	[73]	2015
37	PC$_{71}$BM	SP-BHJ	0.82	13.97	0.70	8.02	[73]	2015
38	SubPc/ SubNc	VP-PHJ	0.96	14.55	0.61	8.4	[74]	2014

Figure 3. Representative oligothiophenes reported during 2011–2015 along with the device parameters and SubPc/SubNc-based NFAs mentioned in this section (circled with a green dashed line).

From the second decade of the 21st century, the structure modification of oligothiophene donors became more concentrated and purposeful. Bäuerle *et al.* systematically investigated DCV end-capped oligothiophenes. Derived from DCV6T (**3**), DCV6T-Bu (**14**) was synthesized and used in VP PHJ OSCs.[62] Owing to a further decreased V_{OC} of 0.81 V and J_{SC} of 4.0 mA cm^{-2}, a low PCE of *ca.* 2.1% was obtained, indicating the importance of the location of alkyl substituents. Comparatively, by adding different alkyl groups to the DCV end-capped quaterthiophene, the PCE of the VP BHJ OSCs improved from 1.5 (**15**) to 2.2 (**17**) and 3.8% (**1**).[63,64] After attempting to use hexathiophenes (**3** and **14**) and tetrathiophene (**15–17**), DCV end-capped pentathiophenes (**2**) were concluded to be better. In 2012, by shortening the n-butyl to methyl groups and tuning the locations of alkylation, Bäuerle *et al.* synthesized three methyl-substituted analogs of DCV5T (**18–20**).[65] Owing to the shortened alkyl groups, all three donors exhibited close π-stacking and red-shifted ultraviolet–visible (UV–VIS) absorptions in thin films, compared

with that of DCV5T (**2**). Among them, **20**:C_{60} blends led to a high PCE of *ca.* 6.9% with a V_{OC} of 0.95 V, J_{SC} of 11.5 mA cm^{-2}, and *FF* of 0.63, which were one of the highest values to date for SM donor-based OSCs. In addition, Bäuerle *et al.* studied the heteroatom effect on the performance of DCV series. Based on the DCV5T molecule (**2**), different numbers of thiophene were replaced by selenophene to form three new donors (**21**–**23**).[66] However, as the number of selenophenes increased, the corresponding V_{OC} declined from 1.02 (**2**) to 0.95 V (**23**), and the three donors exhibited an inferior PCE, compared with that of the DCV5T in the VP BHJ OSCs fabricated with a C_{60} acceptor.

Using fullerene derivatives as acceptors, the light-harvesting of OSCs mainly depended on the absorption of donor molecules. Therefore, broadening the absorption range of oligothiophene donors and improving the J_{SC} was effective for obtaining high PCEs. Fused thiophenes, capable of elevating the HOMO energy level, narrowing the bandgap of corresponding semiconductors, and facilitating charge transport (CT) with a coplanar rigid structure, were aroused in the molecule engineering of oligothiophene donors.[67] In 2014, Bäuerle *et al.* reported the synthesis and characterization of three DCV-substituted S,N-heteropentacene donors (**24**–**26**).[68] Single-junction VP BHJ OSCs fabricated with propyl-attached **24** and C_{60} exhibited a PCE of *ca.* 6.5%, owing to the enhanced J_{SC} of 10.2 mA cm^{-2} and an excellent *FF* of 0.69. They introduced 1-(1,1-dicyanomethylene)-cyclohex-2-ene (DCC), a new terminal group, to the S,N-heteropentacene core to extend the conjugation (**28**).[69] A branched alkyl group (2-ethylhexyl) was attached to the fused-ring core to enhance the solution processability of **28**, and the absorption onset of **28** was successfully extended to nearly 800 nm. The SP **28**:$PC_{61}BM$-based BHJ OSCs exhibited a PCE of *ca.* 4.9% with a V_{OC} of 0.88 V and J_{SC} of 10.8 mA cm^{-2}, which was considerably higher than its DCV end-capped counterpart, **27** (PCE of *ca.* 3.1%).

Other simple fused thiophene derivatives were adopted in a donor design to balance the facile synthesis and narrow bandgap. Bäuerle *et al.* synthesized two dithienopyrrole (DTP)-based SM donors, **29** and **32**; the only difference was the orientation of hexyl groups in bithiophene linkers.[70] This marginal structural tweak led to distinct photophysical and electrochemical properties and a huge PCE gap between the two molecules. The SP **29**:PC$_{61}$BM-based BHJ OSCs exhibited a PCE of *ca.* 4.8% with a V_{OC} of 0.83 V, J_{SC} of 8.8 mA cm^{-2}, and *FF* of 0.66, the **35**:PC$_{61}$BM binary exhibited a low PCE of *ca.* 0.8% with overall reduced parameters (0.72 V, 3.4 mA cm^{-2}, and 0.33). Afterward, a thorough investigation was conducted to elucidate the alkyl group–performance relationship of the DTP-based SM donors. By tuning the branched alkyl chains in the DTP core and the orientation of the hexyl groups in the bithiophene linkers, six DTP-based oligothiophene donors were synthesized (**29**–**34**).[71] All donors were implemented in SP BHJ OSCs demonstrating PCEs between *ca.* 4.4 and 6.1%. Noteworthily, the influence of solvent vapor annealing (SVA) on the morphology of the photoactive layers was systematically investigated, suggesting that exposure to chloroform (CF) vapor reorganized the D:A blend, which increased the absorption and crystallinity of the SM donor, optimizing the morphology and performance. For donor **34**, the as-cast BHJ OSC of **34**:PC$_{61}$BM exhibited a PCE of *ca.* 1.1% with a V_{OC} of 0.817 V, J_{SC} of 4.1 mA cm^{-2}, and FF of 0.32. After 90 s of SVA in CF vapor, a surge in the three parameters (0.843 V, 1.0 mA cm^{-2}, and 0.72) largely enhanced the PCE to *ca.* 6.1%.

Similar to DTP, dithienosilole (DTS) and cyclopentadithiophene (DTC) have been used as electron-rich cores. In 2011, Chen *et al.* reported a DTS-centered, octyl cyanoacetate end-capped donor, DCAO3TSi (**35**).[72] BHJ devices based on DCAO3TSi demonstrated a PCE of *ca.* 5.84% along with a noticeably high *FF* of 0.64. Four years after, DR3TDTS (**37**), the modified version of DCAO3TSi, pushed the PCE to over 8%, while a PCE below 1% was observed for the DTC-based analog, DR3TDTC (**36**).[73] The improved PCE of **37** was

attributed to the use of 3-ethylrhodanine-based terminal groups and an updated posttreatment procedure (thermal annealing (TA) + SVA).

It was noteworthy that, in 2014, when the development of materials and OSC devices moved to solution processing, Knops *et al.* reported an old insoluble molecule, α-6T (**38**), which achieved a new record in VP PHJ OSCs.[74] Using subphthalocyanine (SubPc) and subnaphthalocyanine (SubNc) as electron acceptors (**Figure 3**), a three-layer device of **38**:SubNc:SubPc was fabricated and tested. Attributable to the long-range Förster resonance energy transfer (FRET) and exciton transfer from the outer SubPc to the middle SubNc layer, an extremely high PCE of *ca* 8.4% was achieved for NFA-based OSCs. Although they adopted relatively outdated vacuum processes, these studies revealed the unparalleled advantages of NFAs.

Figure 4. Development and device parameters of donors based on regioregular octylated oligothiophenes.
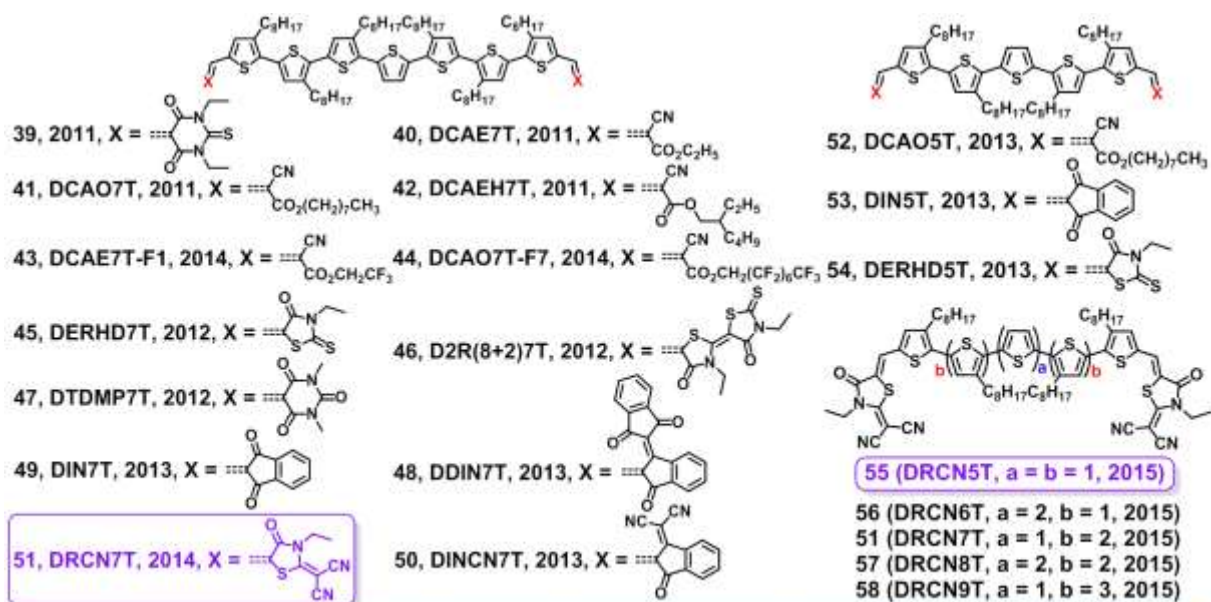
Donor	Acceptor	Device type	V_{OC} (V)	J_{SC} (mA cm^{-2})	FF	PCE (%)	Ref.	Year
39	C_{60}	VP-PHJ	0.51	2.16	0.28	0.36	[77]	2011
40	PC$_{61}$BM	SP-BHJ	0.88	9.94	0.51	4.46	[78]	2011
41	PC$_{61}$BM	SP-BHJ	0.86	10.74	0.55	5.08	[78]	2011
42	PC$_{61}$BM	SP-BHJ	0.93	9.91	0.491	4.52	[78]	2011
43	PC$_{61}$BM	SP-BHJ	0.83	5.5	0.50	2.26	[79]	2014
44	\	\	\	\	\	\	[79]	2014
45	PC$_{61}$BM	SP-BHJ	0.92	13.98	0.474	6.10	[81]	2012
46	PC$_{61}$BM	SP-BHJ	0.92	6.77	0.39	2.46	[85]	2012
47	PC$_{61}$BM	SP-BHJ	0.90	7.54	0.60	4.05	[85]	2012
48	PC$_{61}$BM	SP-BHJ	0.76	3.14	0.28	0.66	[86]	2013
49	PC$_{61}$BM	SP-BHJ	0.80	8.56	0.72	4.93	[86]	2013
50	\	\	\	\	\	\	[86]	2013
51	PC$_{71}$BM	SP-BHJ	0.91	14.87	0.687	9.30	[88]	2014
52	PC$_{61}$BM	SP-BHJ	0.88	7.02	0.53	3.27	[87]	2013
53	PC$_{61}$BM	SP-BHJ	0.78	8.13	0.63	4.00	[87]	2013
54	PC$_{61}$BM	SP-BHJ	1.02	9.26	0.49	4.63	[87]	2013
55	PC$_{71}$BM	SP-BHJ	0.92	15.88	0.69	10.08	[89]	2015
56	PC$_{71}$BM	SP-BHJ	0.92	10.88	0.59	6.33	[89]	2015
57	PC$_{71}$BM	SP-BHJ	0.87	10.98	0.68	6.50	[89]	2015
58	PC$_{71}$BM	SP-BHJ	0.82	13.91	0.69	7.86	[89]	2015

According to previous studies, the highest PCE achieved by single-junction OSCs was reported to be close to 11% during 2011–2015.[75,76] It would be inappropriate to conclude that oligothiophenes had risen only by the PCEs of less than 9% that are previously described. The PCE breakthroughs of oligothiophenes were induced using donors containing regioregular octylated segments (**Figure 4**).

In 2011, Roncali *et al.* reported a thiobarbituric (TB) end-capped septithiophene (**39**).[77] Although it exhibited a narrower bandgap and red-shifted absorption spectrum, compared with those of DCN7T (**13**), the PHJ OSCs of **39**:C_{60} exhibited an inferior PCE of *ca.* 0.36% with a simultaneously decreased V_{OC} of 0.51 V and J_{SC} of 2.16 mA cm^{-2} (*vs.* PCE of *ca.* 1.64% for DCN7T:C_{60}). Subsequently, Chen *et al.* reported a series of cyanoacetate end-capped septithiophenes (**40–42**).[78] These three donors demonstrated high PCEs above 4.5% for SP BHJ OSCs. For the octyl cyanoacetate end-capped DCAO7T (**41**), a PCE of *ca.* 5.08% with a satisfactory V_{OC} of 0.86 V, J_{SC} of 10.74 mA cm^{-2}, and *FF* of 0.55, was achieved based on **52**:$PC_{61}BM$ blends without posttreatment. By incorporating fluorinated alkyl cyanoacetate as terminal groups, Chen *et al.* synthesized two end-fluorinated oligothiophenes, DCAE7T-F1 (**43**) and DCAO7T-F7 (**44**).[79] For DCAE7T-F1, the optimized BHJ OSC devices fabricated with $PC_{61}BM$ exhibited a PCE of *ca.* 2.26% with a V_{OC} of 0.83 V, J_{SC} of 5.50 mA cm^{-2}, and *FF* of 0.50. Compared with DCAE7T (**40**, *ca.* 4.46%), the inferior performance of DCAE7T-F1 could probably be attributed to the excessive D:A phase separation in the blends, which might be due to the aggregation of fluorinated end groups.[80] For DCAO7T-F7, its high lipophobicity prevented its use in BHJ devices.

From DCN7T (**13**) to DCAO7T (**41**), the enhanced PCE was mainly attributed to the drastically improved *FF* of DCAO7T (0.55, *vs.* 0.34 for DCN7T), and a J_{SC} of 10.74 mA cm^{-2}, *vs.* 12.4 mA cm^{-2} for DCN7T. To enhance the PCE of oligothiophenes based on DCAO7T, it was important to increase the J_{SC} without sacrificing V_{OC} or FF. In 2012, Chen *et al.* introduced a new terminal unit, 3-ethylrhodanine, into an octylated septithiophene and formed a new donor molecule, DERHD7T (**45**).[81] Compared with DCAO7T, DERHD7T exhibited a red-shifted absorption and higher molar absorption coefficient, owing to the introduction of rhodanine units; its better light-harvesting capability was successfully expressed in its higher J_{SC} and PCE values. The as-cast BHJ OSCs based on **45**:$PC_{61}BM$ exhibited a PCE of *ca.* 6.1% with a simultaneously enhanced V_{OC} of 0.92 V and J_{SC} of 13.98 mA cm^{-2}. This demonstrated

the huge potential of regioregular octylated oligothiophene-based donors and terminal-group tuning. These studies greatly impacted molecule design strategy; rhodanine derivatives are popular in high-performance SM photovoltaic materials.[82-84]

To screen better terminal groups, various units such as dimerized rhodanine (**46**), barbituric (**47**), and derivatives of 1,3-indandione (**48–50**) have been attached to the octylated septithiophene to build donor molecules.[85,86] None surpassed the PCE of DERHD7T. The 1,3-indandione end-capped donor, DIN7T (**49**), exhibited a relatively better performance. The as-cast BHJ OSCs based on **49**:PC$_{61}$BM exhibited an excellent *FF* of 0.72. However, owing to the decreased J_{SC} (8.21 mA cm^{-2}) and V_{OC} (0.80 V), the PCE was only *ca.* 4.71%. After using 0.3 mg mL^{-1} polydimethylsiloxane (PDMS) as an additive, the J_{SC} slightly increased to 8.56 mA cm^{-2}, but the PCE remained below 5%. In addition to septithiophene, Chen *et al.* investigated the impact of terminal groups on octylated pentathiophenes. According to previous results on septithiophenes, three promising units (octyl cyanoacetate, 3-ethylrhodanine, and 1,3-indandione) were employed to build the corresponding pentathiophene donor (**52–54**).[87] As observed with septithiophenes, rhodanine-flanked DERHD5T (**54**) exhibited the best performance for BHJ OSCs based on **54**:PC$_{61}$BM with a PCE of *ca.* 4.63% (V_{OC} of 1.02 V and J_{SC} of 9.26 mA cm^{-2}).

The existing terminal units appeared incapable of breaking oligothiophene through the PCE bottleneck; therefore, creating new terminal groups became inevitable. In 2014, Chen *et al.* reported a dicyanomethylene substituted rhodanine (RCN) and corresponding RCN flanked donor, DRCN7T (**51**).[88] Regarding the use of classic DCV groups, the RCN was expected to reduce the bandgap of DRCN7T based on DERHD7T (**45**) and enhance electronic coupling between neighboring molecules, which would promote crystallization and facilitate CT.[54] This small change in structure turned good (DERHD7T) to excellent (DRCN7T). Using PC$_{71}$BM as an electron acceptor, DRCN7T-based devices exhibited a PCE as high as
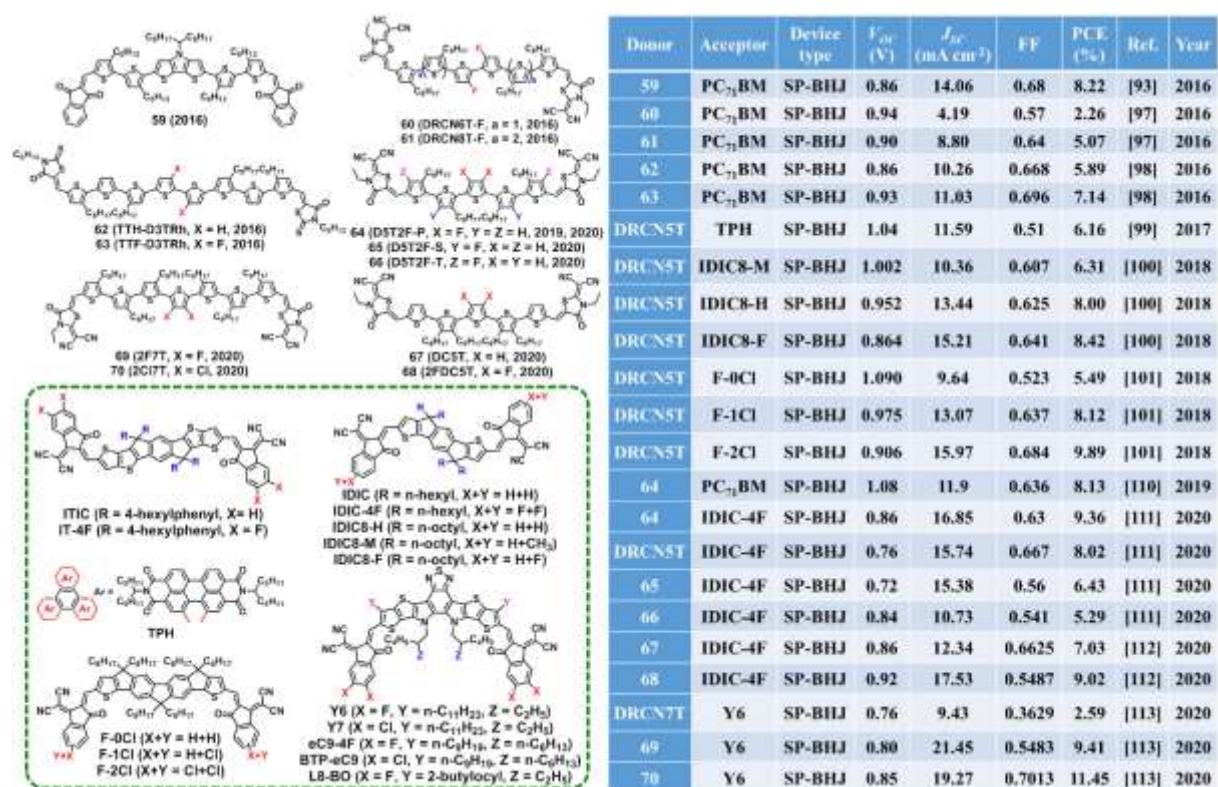
ca. 9.30% with an essentially improved *FF* of 0.69 and J_{SC} of 14.87 mA cm^{-2}. After discovering RCN, Chen *et al.* verified the optimal conjugation length and configuration of regioregular octylated oligothiophenes. A series of SM donors with the same terminal groups (RCN), similar backbones, different conjugation lengths, and spatial symmetry were designed and synthesized.[89] The donor molecule containing an odd number of thiophenes (DRCN5T (**55**), DRCN7T (**51**), and DRCN9T (**58**)) exhibited considerably higher PCE values than those containing an even number of thiophenes (DRCN6T (**56**) and DRCN8T (**57**)). Unexpectedly, the RCN group worked best with the pentathiophene backbone. The BHJ OSCs based on **55**:PC$_{71}$BM exhibited a PCE of *ca.* 10.10%. This is one of the highest PCEs reported for SM donors, thereby rendering the oligothiophene donor parallel to top polymer donors.

During 2011–2015, oligothiophene donors flourished, and the PCEs escalated from below 4% to over 10%. This development was attributed to the effort of molecule designers and constant innovations in device optimization (posttreatment methods, functional additives, electrode interfacial modifications, *etc.*). The emergence of DRCN5T/DRCN7T and their outstanding performance rendered oligothiophenes the protagonist of all SM donors. However, this did not last. Owing to the rise of other SM donors, recurring PCE bottleneck, and birth of the new *era* inaugurated by NFAs, oligothiophenes gradually faded away.

Plateau: 2016–2020

In January 2015, Zhan *et al.* published a paper reporting an NFA molecule, ITIC featured with an indacenodithieno[3,2-b]thiophene (IDTT)-based fused-ring core and 2-(3-oxo-2,3-dihydroinden-1-ylidene)malononitrile (INCN) terminal groups (**Figure 5**).[18] Although many NFAs have been previously published, ITIC essentially changed the entire field of OSC research.[90,91] Compared with traditional fullerene-based acceptors, ITIC represented NFAs with unique advantages, including highly variable molecular structures with easily tunable photophysical and electrochemical properties, broadened and enhanced

absorption in the visible and near-infrared (NIR) regions, and low driving force for charge separation.[92] OSC research officially entered a new *era*. Unfortunately, dissimilar to competitive SM donors that quickly adapted to NFAs and exhibited significantly improved PCEs, oligothiophene donors and NFAs experienced a long and painful run-in period. In fullerene systems, the PCE bottleneck reappeared for oligothiophene donors.

| Donor	Acceptor	Device type	V_{OC} (V)	J_{SC} (mA cm^{-2})	FF	PCE (%)	Ref.	Year
59	PC$_{71}$BM	SP-BHJ	0.86	14.06	0.68	8.22	[93]	2016
60	PC$_{71}$BM	SP-BHJ	0.94	4.19	0.57	2.26	[97]	2016
61	PC$_{71}$BM	SP-BHJ	0.90	8.80	0.64	5.07	[97]	2016
62	PC$_{71}$BM	SP-BHJ	0.86	10.26	0.668	5.89	[98]	2016
63	PC$_{71}$BM	SP-BHJ	0.93	11.03	0.696	7.14	[98]	2016
DRCN5T	TPH	SP-BHJ	1.04	11.59	0.51	6.16	[99]	2017
DRCN5T	IDIC8-M	SP-BHJ	1.002	10.36	0.607	6.31	[100]	2018
DRCN5T	IDIC8-H	SP-BHJ	0.952	13.44	0.625	8.00	[100]	2018
DRCN5T	IDIC8-F	SP-BHJ	0.864	15.21	0.641	8.42	[100]	2018
DRCN5T	F-0Cl	SP-BHJ	1.090	9.64	0.523	5.49	[101]	2018
DRCN5T	F-1Cl	SP-BHJ	0.975	13.07	0.637	8.12	[101]	2018
DRCN5T	F-2Cl	SP-BHJ	0.906	15.97	0.684	9.89	[101]	2018
64	PC$_{71}$BM	SP-BHJ	1.08	11.9	0.636	8.13	[110]	2019
64	IDIC-4F	SP-BHJ	0.86	16.85	0.63	9.36	[111]	2020
DRCN5T	IDIC-4F	SP-BHJ	0.76	15.74	0.667	8.02	[111]	2020
65	IDIC-4F	SP-BHJ	0.72	15.38	0.56	6.43	[111]	2020
66	IDIC-4F	SP-BHJ	0.84	10.73	0.541	5.29	[111]	2020
67	IDIC-4F	SP-BHJ	0.86	12.34	0.6625	7.03	[112]	2020
68	IDIC-4F	SP-BHJ	0.92	17.53	0.5487	9.02	[112]	2020
DRCN7T	Y6	SP-BHJ	0.76	9.43	0.3629	2.59	[113]	2020
69	Y6	SP-BHJ	0.80	21.45	0.5483	9.41	[113]	2020
70	Y6	SP-BHJ	0.85	19.27	0.7013	11.45	[113]	2020

Figure 5. Representative oligothiophenes reported during 2016–2020 with the device parameters and other NFAs mentioned in this paper (circled with a green dashed line).

After achieving a PCE exceeding 10%, researchers sought promising structures of oligothiophenes in fullerene systems. Based on previously reported DTP-centered donor, **33**, Mishra *et al.* synthesized a 1,3-indandione end-capped analog, **59**.[93] By adopting the two-step annealing (TA followed by SVA), the SP BHJ OSCs of the **59**:PC$_{71}$BM binary exhibited a PCE of *ca.* 8.22% with a well-balanced V_{OC} of 0.86 V and J_{SC} of 14.06 mA cm^{-2}. In polymer donor designing, halogenation, particularly fluorination, has been widely used because it was confirmed that fluorination is an effective pathway to tune the intramolecular

and/or intermolecular interactions of the conjugated backbone of polymer donors, thereby affecting their photovoltaic performance.[94-96] Adopting the fluorination strategy, Chen *et al.* synthesized two backbone fluorinated molecules, DRCN6T-F (**60**) and DRCN6T-F (**61**) in 2016.[97] Compared with their nonfluorinated counterparts, DRCN6T (**56**) and DRCN8T (**57**), **60** and **61** exhibited enhanced intermolecular interactions and deepened HOMO energy levels, which were attributed to the improved V_{OC}. However, owing to the drastically declining J_{SC}, the device performance based on **60**:$PC_{71}BM$ and **61**:$PC_{71}BM$ were merely *ca.* 2.26 and 5.07% (*vs.* 6.33% for DRCN6T and 6.37% for DRCN8T), respectively. Peng *et al.* reported a fluorinated donor, TTF-D3TRh (**63**) in 2016.[98] The fluorination endowed TTF-D3TRh with a lower HOMO level, better molecular stacking, and higher mobility, compared with those of nonfluorinated TTH-D3TRh (**62**). The as-cast BHJ OSCs based on **63**:$PC_{71}BM$ exhibited a satisfactory PCE of *ca.* 5.80%. After employing the inverted device architecture, the corresponding OSCs exhibited largely elevated PCEs of *ca.* 7.14% for donor **77**.

By examining the parameters of oligothiophene:fullerene-based OSCs (**Figures 2–5**), to break the PCE ceiling of oligothiophene donors, the relatively low J_{SC} (< 16 mA cm^{-2}) was the "shortest board" that needed urgent attention. To broaden the absorption and light-harvesting range of the D:A blend and enhance the corresponding J_{SC}, researchers naturally turned to NFAs, which exhibit strong NIR absorption. In 2017, Wang *et al.* combined DRCN5T (**55**) with a perylene diimide (PDI)-based NFA, **TPH**, to fabricate the all-SM (ASM) OSCs.[99] With simple TA, the devices exhibited a PCE of *ca.* 6.16% with a high V_{OC} of 1.04 V but medium J_{SC} of 11.59 mA cm^{-2}. Although this PCE was among the highest for NFA-based ASM OSCs to date, it was considerably worse than that of the DRCN5T:$PC_{71}BM$ binary. Next, Chen *et al.* employed a series of ITIC-derived NFAs to fabricate ASM OSCs with DRCN5T. In 2018, three NFAs, **IDIC8-M**, **IDIC8-H**, and **IDIC8-F** with an alkylated indaceno[1,2-b:5,6-b']dithiophene (IDT) unit as the central core and INCN or its derivatives as terminal groups were synthesized as NFAs to construct ASM OSCs with DRCN5T.[100]

The fluorinated **IDIC8-F** exhibited a red-shifted absorption spectrum, compared with the other counterparts, and was more complementary with the absorption range of DRCN5T. The devices based on DRCN5T**:IDIC8-F** demonstrated the best PCE of *ca.* 8.42% with a high J_{SC} of 15.21 mA cm^{-2}. Subsequently, Chen *et al.* reported another series of NFAs (**F-0Cl**, **F-1Cl**, and **F-2Cl**) with an alkylated fluorine core and INCN or its chlorinated derivatives as terminal groups, and the devices were obtained from the DRCN5T**:F-2Cl** binary.[101] Compared with the DRCN5T**:IDIC8-F** combination, DRCN5T**:F-2Cl** exhibited overall enhanced parameters in ASM OSC devices (**Table 4**). Consequently, a high PCE of *ca.* 9.89% was obtained for oligothiophene-based NFA OSCs, which was inferior to the performance of the DRCN5T:PC$_{71}$BM binary.
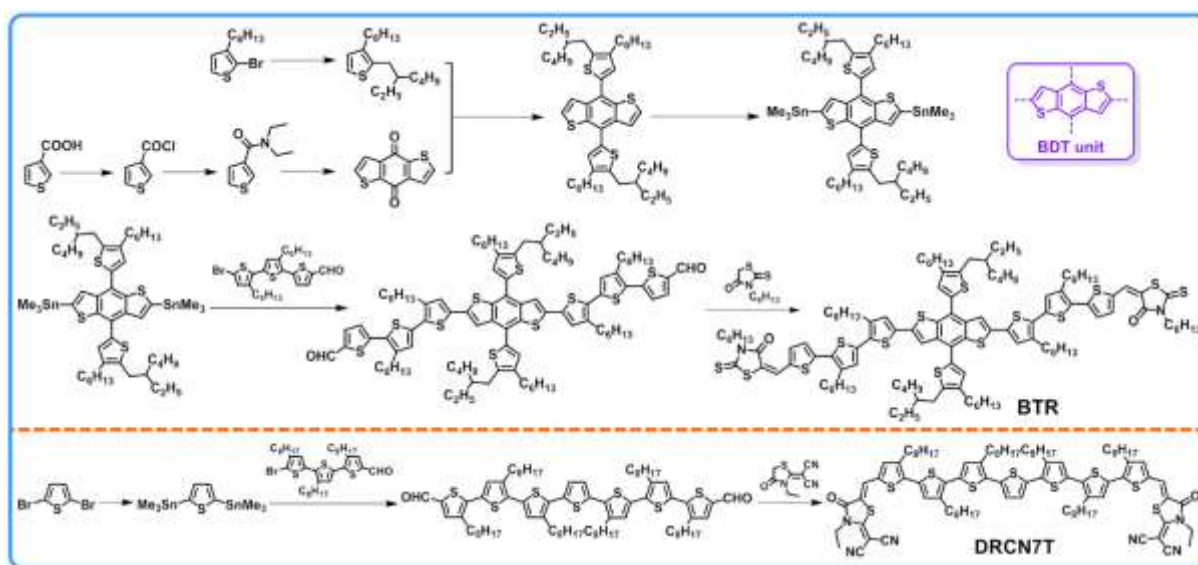
Figure 6. Synthetic routes of benzodithiophene (BDT) donor, **BTR** (top), and oligothiophene donor, **DRCN7T** (bottom).

Oligothiophene donors were being developed to improve their PCE; however, competitors had already risen with the help of NFAs. Derived from fused thiophenes and emerging in the late 2000s, benzodithiophene (BDT) is one of the most successful building blocks in the design of high-performance organic photovoltaic materials.[102,103] As a latecomer, BDT-based SM donors did not demonstrate conspicuous advantages in performance in the *era* of fullerene acceptors. In 2015, Jones *et al.* reported a representative

BDT-based SM donor, BTR.[104] The SP BHJ OSCs based on BTR:PC$_{71}$BM demonstrated a high PCE of *ca.* 9.3% with an excellent *J*$_{SC}$ of 13.40 mA cm^{-2} and *FF* of 0.77, which was identical with the PCE of the DRCN7T:PC$_{71}$BM binary. As observed from the structures and synthetic routes of BTR and DRCN7T (**Figure 6**), although they shared extremely similar π-linkers, terminal groups, and photovoltaic performance in fullerene systems, the facile synthesis of the central unit significantly decreased the time cost and raw material cost when synthesizing DRCN7T.

Regrettably, the situation has changed since NFAs arose. When DRCN5T was reported to work with **TPH** and exhibited a medium PCE of *ca.* 6.16%, the BDT-based SM donor had achieved a PCE of over 10% in **IDIC**-based BHJ OSCs[105]. Before the PCE of *ca.* 9.89% was achieved using the DRCN5T:**F-2Cl** binary, the PCE of the BDT SM donor and NFA binary already surpassed 11% with a high *J*$_{SC}$ of over 18 mA cm^{-2}.[106] After the star NFA, Y6, was invented, the PCE gap between BDT donors and oligothiophenes widened.[21, 82, 107-109] Oligothiophenes suffered repeated failures in NFA systems while BDT donors improved the PCE of ASM OSCs. As a result, oligothiophene was stuck in limbo, and BDT-based structures were preferred when developing new SM donors. This situation led to serious homogeneity in developing high-performance SM and severely constrained the innovation and development of photovoltaic materials.

In 2019, our group reported a centrally fluorinated analog of DRCN5T, D5T2F-P (**64**).[110] Compared with DRCN5T, the fluorinated donor exhibited deepened HOMO energy levels, broadened bandgap, and ordered molecular packing. The devices fabricated with **64**:PC$_{71}$BM led to a PCE of *ca.* 8.30% with an unexpectedly high *V*$_{OC}$ of 1.08 V. Although the PCE of **64** was limited by the decreased *J*$_{SC}$ (11.9 mA cm^{-2}) attributed to the narrowed absorption, compared with DRCN5T, the outstanding *V*$_{OC}$ and blue-shifted absorption spectrum rendered it promising for cooperation with ITIC-like NIR NFAs.

Afterward, based on D5T2F-P (**64**), our group reported two other difluorinated isomers, (D5T2F-S (**65**) and D5T2F-T (**66**)), to investigate the positional isomeric effect of fluorine substitution on performance variations of NFA-based OSCs.[111] The introduction of fluorine was demonstrated to affect the photophysical, electrochemical, and aggregation properties of the donor molecules, compared with the nonfluorinated DRCN5T. Importantly, the locations of fluorine substitution significantly influenced the conformer disorder, donor–acceptor complex binding energy, and exciton binding energy, causing distinct variations in the device performances of the three isomer-based NFA OSCs. Combined with **IDIC-4F**, the highest PCE of *ca.* 9.36% with a J_{SC} of 16.85 mA cm^{-2} and V_{OC} of 0.86 V was achieved using **64**:**IDIC-4F**-based devices, which exhibited simultaneously enhanced properties, compared with those of DRCN5T:**IDIC-4F**-based devices (PCE of *ca.* 8.02%, J_{SC} of 15.74 mA cm^{-2}, and V_{OC} of 0.76 V).

This previous study appeared to be the "silver lining" in the development of oligothiophene donors. Although there was a wide PCE gap between the BDT donor (PCE, approximately 15%) and oligothiophene (PCE, approximately 10%), at least central fluorination appeared to be a feasible pathway to design better donors than DRCN5T in NFA systems. Our group reported another SM donor, DC5T (**67**) along with its fluorinated counterpart, 2FDC5T (**68**).[112] Compared with DRCN5T/D5T2F-P, the only structural difference of DC5T/2FDC5T was the use of the dialkylated thienyl unit. Similarly, the fluorinated donor, **68**, exhibited better performances in NFA-based BHJ OSCs, compared with that of **67**. A PCE of *ca.* 9.02% was achieved using the **67**:**IDIC-4F** binary with a satisfactory V_{OC} of 0.92 V and J_{SC} of 17.53 mA cm^{-2}.

Subsequently, our group synthesized 2F7T (**69**), the centrally difluorinated analog of DRCN7T, and used it to fabricate NFA-based OSCs.[113] With **Y6**, a PCE of *ca.* 9.41% was exhibited with a satisfactory J_{SC} of 21.45 mA cm^{-2}, medium V_{OC} of 0.80 V, and *FF* of 0.548.

Inspired by studies on chlorinated donors and NFAs, our group synthesized a centrally chlorinated donor, 2Cl7T (**70**). When 2Cl7T was combined with **Y6**, a high PCE of *ca.* 11.45% was exhibited with a well-balanced V_{OC} of 0.85 V, J_{SC} of 19.27 mA cm^{-2}, and *FF* of 0.701. Apart from a deeper HOMO energy level, 2Cl7T exhibited optimal balance between crystallinity and miscibility with **Y6** in blend films, compared with the other two counterparts (DRCN7T with a PCE of *ca.* 2.5% and **69**).

From 2016 to 2020, the rise of NFAs and the decline of oligothiophenes occurred. Fortunately, at the beginning of the second decade of the 21st century, the bottoming out of oligothiophenes commenced. In state-of-the-art NFA systems (**Y6, eC9-4F, *etc*.**), it could be speculated that instead of the traditional A–π–D–π–A structure (DRCN7T), the A–π–A'–π–A-featured septithiophene (2Cl7T) was probably a more suitable design for high-performance donors. Although they lagged far behind top BDT-based SM donors in terms of the PCE, the revival of oligothiophenes was anticipated.

Revival: new design and new role
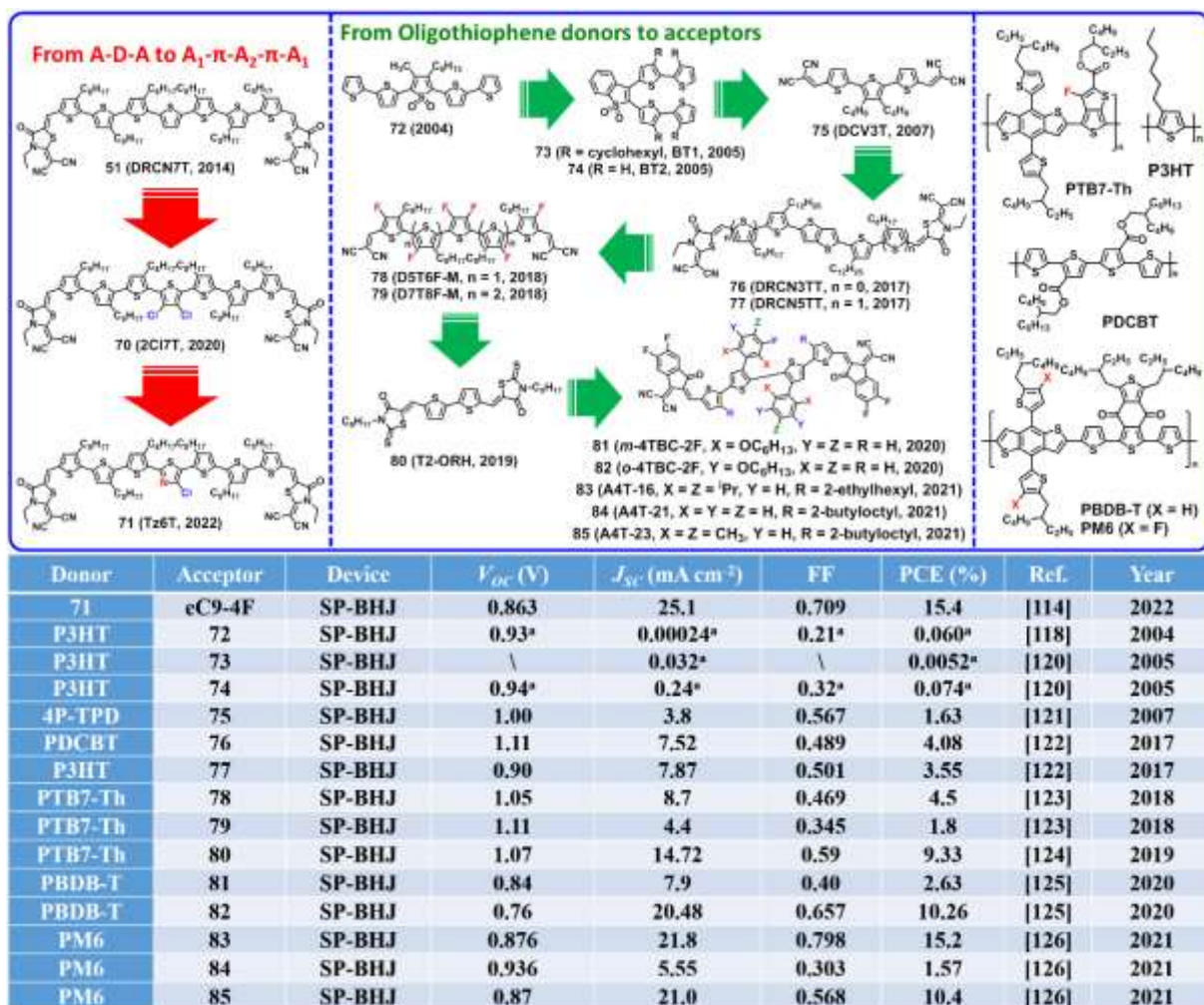
Figure 7. New design strategies for high-performance oligothiophene donors/acceptors with the device parameters and polymer donors mentioned in this paper.

[a] Characterized under 80 mW cm^{-2} white light illumination.

Donor	Acceptor	Device	V_{OC} (V)	J_{SC} (mA cm^{-2})	FF	PCE (%)	Ref.	Year
71	eC9-4F	SP-BHJ	0.863	25.1	0.709	15.4	[114]	2022
P3HT	72	SP-BHJ	0.93[a]	0.00024[a]	0.21[a]	0.060[a]	[118]	2004
P3HT	73	SP-BHJ	\	0.032[a]	\	0.0052[a]	[120]	2005
P3HT	74	SP-BHJ	0.94[a]	0.24[a]	0.32[a]	0.074[a]	[120]	2005
4P-TPD	75	SP-BHJ	1.00	3.8	0.567	1.63	[121]	2007
PDCBT	76	SP-BHJ	1.11	7.52	0.489	4.08	[122]	2017
P3HT	77	SP-BHJ	0.90	7.87	0.501	3.55	[122]	2017
PTB7-Th	78	SP-BHJ	1.05	8.7	0.469	4.5	[123]	2018
PTB7-Th	79	SP-BHJ	1.11	4.4	0.345	1.8	[123]	2018
PTB7-Th	80	SP-BHJ	1.07	14.72	0.59	9.33	[124]	2019
PBDB-T	81	SP-BHJ	0.84	7.9	0.40	2.63	[125]	2020
PBDB-T	82	SP-BHJ	0.76	20.48	0.657	10.26	[125]	2020
PM6	83	SP-BHJ	0.876	21.8	0.798	15.2	[126]	2021
PM6	84	SP-BHJ	0.936	5.55	0.303	1.57	[126]	2021
PM6	85	SP-BHJ	0.87	21.0	0.568	10.4	[126]	2021

The development of 2F7T (**69**) and 2Cl7T (**70**) provided guidelines for the development of oligothiophene-based donors with superior device performance. Based on the structure of 2Cl7T, another A–π–A'–π–A-structured oligothiophene, Tz6T (**71**), was synthesized. Owing to the introduction of unsymmetric chlorinated thiazole, a more electron-negative moiety than dichlorothiophene, **71** demonstrated blue-shifted absorption spectra, deepened HOMO levels, and improved crystallinity, compared with those of its predecessor, **70**.[114] After use as donor material in the OSCs with an NFA, **eC9-4F**[115], a PCE of 15.4% was achieved using the **71:eC9-4F** binary with a V_{OC} of 0.863 V, J_{SC} of 25.1 mA cm^{-2}, and *FF* of 0.709. Under the same conditions, the **70:eC9-4F** binary exhibited a considerably low

PCE of *ca.* 12.55%. This result narrowed the PCE gap between oligothiophenes and BDT donors and confirmed that oligothiophenes were promising candidates for scale-up productions and applications of OSCs (**Figure 8**).
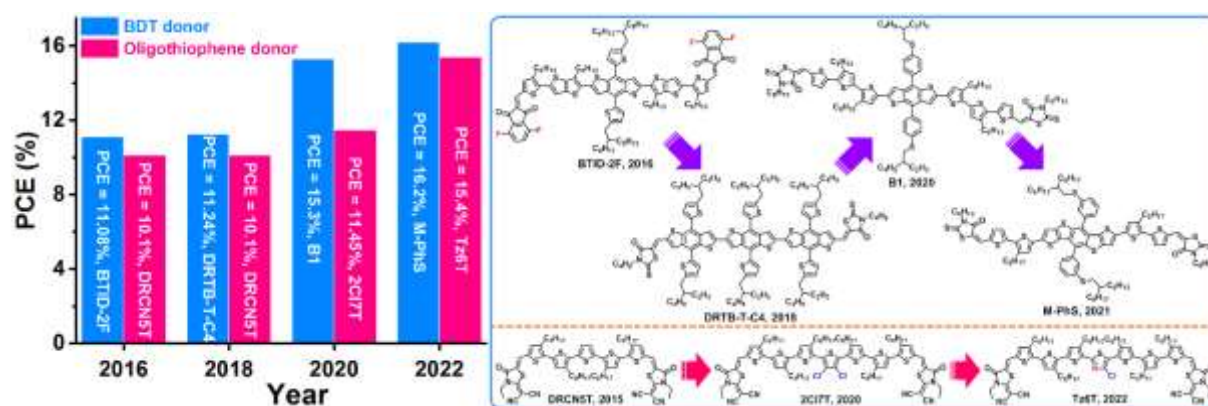
Figure 8. Comparison of the PCEs achieved using oligothiophene donor and BDT donor-based binary OSCs in the last six years with the aforementioned molecules.[89, 106, 107, 113, 114, 116, 117]

Apart from traditional electron donors, oligothiophene-based acceptors were revitalized in the second decade of the 21st century. Although to play a relatively obscure role in OSCs, the oligothiophene-based acceptors had already been reported in the mid-2000s. Camaioni *et al.* reported a series of oligothiophene-S,S-dioxides (**72**–**74**) and investigated their photovoltaic properties as electron acceptors in SP BHJ OSCs.[118-120] However, these materials exhibited only negligible PCEs ($< 0.1\%$) with a nearly undetectable J_{SC} ($< 10^{-3}$ mA cm^{-2}). In 2006, Bäuerle *et al.* reported a DCV end-capped terthiophene, DCV3T (**75**).[121] With an electron donor, N,N,N',N'-tetraphenyl[1,1':4',1'':4'',1'''-quaterphenyl]-4,4'''-diamine (4P-TPD), **75**-based devices exhibited a satisfactory PCE of *ca.* 1.63%; **75** cooperated with more electron-negative C$_{60}$ and functioned as an electron donor. The corresponding PHJ OSCs exhibited a comparable PCE of *ca.* 1.69%. This demonstrated that it was unprofitable to categorize an organic semiconductive molecule as an electron donor or acceptor isolatedly; it depended on the HOMO/LUMO energy levels of the counterpart.

In the next 10 years, owing to the unmatched performance of fullerene acceptors, the oligothiophene-based acceptors received minimal attention. In 2017, Chen *et al.* demonstrated that SM donors, DRCN3TT (**76**) and DRCN5TT (**77**), could function as electron acceptors. With classic polymer donors, **P3HT** and **PDCBT**, **90** exhibited PCEs of *ca.* 3.55 and 4.08%, respectively.[122] Our group synthesized two highly fluorinated oligothiophenes, D5T6F-M (**78**) and D7T8F-M (**79**).[123] Owing to the introduction of multiple fluorine atoms, these two molecules exhibited highly deepened HOMO/LUMO energy levels, which made them capable as wide bandgap acceptors. The BHJ OSCs based on **78** and a low bandgap polymer donor, PTB7-Th, exhibited a PCE of *ca.* 4.5% with a high V_{OC} of 1.05 V, and the devices of **79**:PTB7-Th exhibited an inferior PCE of *ca.* 1.8% because of their more rigid structure and consequent poor solubility. In 2019, Lim *et al.* synthesized a rhodanine-flanked bithiophene, T2-ORH (**80**).[124] With this low cost wide bandgap NFA, a high PCE of *ca.* 9.33% with a V_{OC} of 1.07 V and J_{SC} of 14.72 mA cm^{-2} was achieved using PTB7-Th-based OSCs under simple additive-free fabrication conditions. This study demonstrated the best result of oligothiophene-based acceptors to date and attracted attention to these long-forgotten NFAs.

In 2020, inspired by previous studies on ITIC-derived and oligothiophene-based NFAs, Bo *et al.* reported the *De Novo* design of two tetrathiophene-based NFAs with completely nonfused structures.[125] Attached to isomeric phenyl side chains, *o*-4TBC-2F (**81**) and *m*-4TBC-2F (**82**) exhibited distinct properties; the former had a planar backbone and exhibited a more ordered molecular orientation and stacking in the films after TA, while the latter had a twisted structure and did not respond to TA. Owing to the better CT endowed by the structure of **82**, a PCE of *ca.* 10.26% was achieved using the PBDB-T:**82** binary with a high J_{SC} of 20.48 mA cm^{-2}, while the PBDB-T:**81** binary exhibited a low PCE of *ca.* 2.63%. Afterward, Hou *et al.* reported the optimized versions of NFA **82**, A4T-16 (**83**), A4T-21 (**84**), and A4T-23 (**85**) in 2021.[126] By tuning the phenyl groups in the central bithiophene unit and the branched alkyl group in the adjacent thiophenes, three oligothiophene NFAs exhibited

different optoelectronic properties. The corresponding optical bandgap varied from 1.43 eV (for **85**) to 1.66 eV (**84**). Using a 2,4,6-trimethylphenyl substituent and a 2-ethylhexyl alkyl group, the resulting NFA, **83**, exhibited the best balanced intramolecular CT and intermolecular packing. Thus, the PM6:**83**-based OSCs exhibited a PCE of *ca.* 15.2%, which was the highest value achieved for devices based on oligothiophene-based NFAs. It paved the way for the design of low cost high-performance nonfused NFAs.

Overall, after over five years of investigating and exploring, oligothiophene-based photovoltaic materials have begun to attract attention because of unrelenting innovations in molecular designs and the consequent revival of oligothiophene donors and acceptors. Relevant studies are ongoing.

Summary and outlook

Herein, the phylogeny of oligothiophene-based organic photovoltaic materials, particularly the development process of electron donors, has been revisited. PCEs exceeding 15% have placed oligothiophene donors/acceptors at the forefront of SM donors/acceptors, but the high PCEs that approach or exceed 20% are strongly desirable for research and industrial communities. After reviewing these reported molecules, new inspirations were obtained from the perspective of molecular engineering as follows:

(1) For oligothiophene donors, it was observed that compared with the classic A–π–D–π–A design, adopting the A–π–A'–π–A configuration was more effective for synthesizing high-performance oligothiophene donors. Moreover, combining DFT calculations and the experimental characterization results of Tz6T, the following semiempirical rules can be summarized for the further improvement of oligothiophene donor-based OSCs:

First, introducing a certain electron-withdrawing moiety as the central unit of the oligothiophene is important. It can reduce the HOMO energy level of the donor, enhance the

V_{OC} of devices, and generate a repulsion force to the electron-negative terminal groups of commonly used NFAs, which leads to reduced charge recombination. Judging from the HOMO energy levels of **Tz6T** (−5.35 eV) and NFA **eC9-4F** (−5.77 eV), a considerable gap exists between this D/A combination, which could be used to scavenge additional V_{OC}. Secondly, apart from inserting an electron-withdrawing functional group, the unsymmetric central unit could reinforce the intramolecular CT feature of the donor, which would facilitate charge separation. Finally, a carefully selected NFA is as pivotal as a delicately designed donor for the PCE enhancement. When optimizing Tz6T-based devices, our group started with the most adopted NFA, **Y6**. However, the **Tz6T**:**Y6** blends only exhibited a PCE of *ca.* 13.55%. During the following study, we attempted to use other **Y6**-derived NFAs, such as **Y7**, **BTP-eC9**, and **L8-BO** (**Figure 5**). Fortunately, the most compatible NFA, **eC9-4F**, and more inspiring and enlightening results were obtained.

(2) For oligothiophene acceptors, although relevant studies have just commenced, which are unable to challenge the dominant position of Y-series NFAs presently, enormous potential exists in these newcomers. For A4T-16 (**97**), the bandgap is approximately 1.45 eV, and the absorption onset of thin films is *ca.* 855 nm, which is far from ideal, compared with Y-series NIR NFAs (for Y6, the bandgap is approximately 1.33 eV, and the absorption onset of the thin film is *ca.* 931 nm). If the light-harvesting range of **A4T-16** and the corresponding J_{SC} in devices can be increased while maintaining a satisfactory V_{OC} and *FF*, the resulting PCEs would be extremely promising. Similarly, we believe that the screening of donor materials and a delicate morphology control of D:A blends (*e.g.,* side chain adjustment of donor/acceptor and additive-induced miscibility tuning) are essential for improving the PCE.

(3) In addition, owing to the emergence of high-performance oligothiophene acceptors, the combination of oligothiophene donor/acceptors, *i.e.*, all-oligothiophene (AOT) OSCs has become a new research topic full of possibilities. With the potential of reducing the synthetic

complexity and cost of ASM OSCs, AOT OSCs will be highly competitive if the corresponding PCEs are elevated to the state-of-the-art level (*ca.* 16% of ASM OSCs based on BDT donors and Y-series NFAs).

Conflict of interest

The authors declare no conflict of interest.

Acknowledgements

References

[1] Lewis, N. S. (2007) Toward Cost-Effective Solar Energy Use. *Science* 315, 798–801.

[2] Jordan, D. *et al.* (2021) Build solar-energy systems to last — save billions. *Nature* 600, 215–217.

[3] Huang, Y. *et al.* (2014) Bulk Heterojunction Solar Cells: Morphology and Performance Relationships. *Chem. Rev.* 114, 7006–7043.

[4] Lu, L. *et al.* (2015) Recent Advances in Bulk Heterojunction Polymer Solar Cells. *Chem. Rev.* 115, 12666–12731.

[5] Li, G. *et al.* (2017) Low-bandgap conjugated polymers enabling solution-processable tandem solar cells. *Nat. Rev. Mater.* 2, 17043.

[6] Liu, C. *et al.* (2016) Low bandgap semiconducting polymers for polymeric photovoltaics, *Chem. Soc. Rev* 45, 4825–4846.

[7] Yao, H. *et al.* (2016) Molecular Design of Benzodithiophene-Based Organic Photovoltaic Materials. *Chem. Rev* 116, 7397–7457.

[8] Tang, C. W. *et al.* (1986) Two-layer organic photovoltaic cell. *Appl. Phys. Lett* 48, 183–185.

[9] Mishra A. *et al.* (2012) Small Molecule Organic Semiconductors on the Move: Promises for Future Solar Energy Technology. *Angew. Chem. Int. Ed* 51, 2020–2067.

[10] Yu, G. *et al.* (1995) Polymer Photovoltaic Cells: Enhanced Efficiencies via a Network of Internal Donor-Acceptor Heterojunctions. *Science* 270, 1789–1791.

[11] Halls, J. J. M. *et al.* (1995) Efficient photodiodes from interpenetrating polymer networks. *Nature* 376, 498–500.

[12] Arunagiri L. *et al.* (2020) Selective Hole and Electron Transport in Efficient Quaternary Blend Organic Solar Cells. *Joule* 4, 1790–1805.

[13] Gunes, S. *et al.* (2007) Conjugated Polymer-Based Organic Solar Cells. *Chem. Rev* 107, 1324–1338.

[14] Park, S. *et al.* (2020) Progress in Materials, Solution Processes, and Long-Term Stability for Large-Area Organic Photovoltaics. *Adv. Mater* 32, 2002217.

[15] Liu, H. *et al.* (2021) Technical Challenges and Perspectives for the Commercialization of Solution-Processable Solar Cells. *Adv. Mater. Technol* 6, 2000960.

[16] Liang, Y. *et al.* (2009) Development of New Semiconducting Polymers for High Performance Solar Cells. *J. Am. Chem. Soc.* 131, 56–57.

[17] Li, G. *et al.* (2006) Efficient Inverted Polymer Solar Cells. *Appl. Phys. Lett.* 88, 253503.

[18] You, J. B. *et al.* (2013) A polymer tandem solar cell with 10.6% power conversion efficiency. *Nat. Commun.* 4:1446.

[19] Zhang, Y. *et al.* (2021) Graded bulk-heterojunction enables 17% binary organic solar cells via nonhalogenated open air coating. *Nat. Commun.* 12:4815.

[20] Lin, Y. *et al.* (2015) An Electron Acceptor Challenging Fullerenes for Efficient Polymer Solar Cells. *Adv. Mater* 27, 1170–1174.

[21] Zhang, G. Y. *et al.* (2018) Nonfullerene Acceptor Molecules for Bulk Heterojunction Organic Solar Cells. *Chem. Rev* 118, 3447–3507.

[22] Yan, C. *et al.* (2018) Non-fullerene acceptors for organic solar cells. *Nat. Rev. Mater* 3, 18003.

[23] Yuan, J. *et al.* (2019) Single-Junction Organic Solar Cell with over 15% Efficiency Using Fused-Ring Acceptor with Electron-Deficient Core. *Joule* 3, 1140–1151.

[24] Cui, Y. *et al.* (2020) Single-Junction Organic Photovoltaic Cells with Approaching 18% Efficiency. *Adv. Mater* 32, 1908205.

[25] Wang, J. Y. *et al.* (2021) Fused-Ring Electron Acceptors for Photovoltaics and Beyond. *Acc. Chem. Res* 54, 132–143.

[26] Yuan, J. *et al.* (2019) Enabling low voltage losses and high photocurrent in fullerene-free organic photovoltaics. *Nat. Commun.* 10:570.

[27] Li, C. *et al.* (2021) Non-fullerene acceptors with branched side chains and improved molecular packing to exceed 18% efficiency in organic solar cells. *Nat. Energy* 6, 605–613.

[28] Cai, Y. H. *et al.* (2021) A Well-Mixed Phase Formed by Two Compatible Non-Fullerene Acceptors Enables Ternary Organic Solar Cells with Efficiency over 18.6%. *Adv. Mater.* 33, 2101733.

[29] B, P. Q. *et al.* (2021) Reduced non-radiative charge recombination enables organic photovoltaic cell approaching 19% efficiency. *Joule* 5, 2408–2419.

[30] Cui, C. H. *et al.* (2015) High-Performance Organic Solar Cells Based on a Small Molecule with Alkylthio-Thienyl-Conjugated Side Chains without Extra Treatments. *Adv. Mater.* 27, 7469–7475.

[31] Gupta, V. *et al.* (2013) Barium: An Efficient Cathode Layer for Bulk-heterojunction Solar Cells. *Adv. Mater.* 25, 2397–2402.

[32] Gao, K. *et al.* (2015) Deep absorbing porphyrin small molecule for high-performance organic solar cells with very low energy losses. *J. Am. Chem. Soc.* 137, 7282–7285.

[33] Kan, B. *et al.* (2017) A simple small molecule as the acceptor for fullerene-free organic solar cells. *Sci. China Chem.* 60, 366–369.

[34] Lin, Y. *et al.* (2016) Fluorination-substitution effect on all-small-molecule organic solar cells. *Acc. Chem. Res.* 49, 175–183.

[35] Huo, Y. *et al.* (2019) Nonfullerene all-small-molecule organic solar cells. *ACS Energy Lett.* 4, 1241–1250.

[36] Perepichka, I. F. *et al.* (2019) Handbook of Thiophene-Based Materials: Applications in Organic Electronics and Photonics. John Wiley & Sons, Ltd.

[37] Noma, N. *et al.* (1995) αThiophene octamer as a new class of photo-active material for photoelectrical conversion. *Adv. Mater.* 7, 647–648.

[38] Ni, W. *et al.* (2015) A-D-A small molecules for solution-processed organic photovoltaic cells. *Chem. Commun.* 51, 4936–4950.

[39] Weu, A. *et al*. (2019) Energy Transfer to a Stable Donor Suppresses Degradation in Organic Solar Cells. *Adv. Funct. Mater.* 30, 1907432.

[40] Tanaka, S. *et al*. (2011) Synthesis of Well-Defined Head-to-Tail-Type Oligothiophenes by Regioselective Deprotonation of 3-Substituted Thiophenes and Nickel-Catalyzed Cross-Coupling Reaction. *J. Am. Chem. Soc.* 133, 16734–16737.

[41] Tanaka, S. *et al*. (2012) Concise synthesis of well-defined linear and branched oligothiophenes with nickel-catalyzed regiocontrolled cross-coupling of 3-substituted thiophenes by catalytically generated magnesium amide. *Chem. Eur. J.* 19, 1658–1665.

[42] Dang, M. T. *et al*. (2011) P3HT: PCBM, Best Seller in Polymer Photovoltaic Research. *Adv. Mater.* 23, 3597–3602.

[43] Wan, X. *et al*. (2020) Acceptor-donor-acceptor type molecules for high performance organic photovoltaics - chemistry and mechanism. *Chem. Soc. Rev.* 49, 2828–2842.

[44] Mishra, A. *et al*. (2009) Functional oligothiophenes: molecular design for multidimensional nanoarchitectures and their applications. *Chem. Rev.* 109, 1141–1276.

[45] Wang, J. *et al*. (2016) Triarylamine: Versatile Platform for Organic, Dye-Sensitized, and Perovskite Solar Cells. *Chem. Rev.* 116, 14675–14725.

[46] Li, W. *et al*. (2016) Diketopyrrolopyrrole Polymers for Organic Solar Cells. *Acc. Chem. Res.* 49, 78–85.

[47] Yao, H. *et al*. (2016) Molecular Design of Benzodithiophene-Based Organic Photovoltaic Materials. *Chem. Rev.* 116, 7397−7457.

[48] Timpel, M. *et al.* (2020) Oligothiophene-Based Phosphonates for Surface Modification of Ultraflat Transparent Conductive Oxides. *Adv. Mater. Interfaces* 7, 1902114.

[49] Planells, M. *et al.* (2014) A Quarterthiophene-Based Dye as an Efficient Interface Modifier for Hybrid Titanium Dioxide/Poly(3-hexylthiophene)(P3HT) Solar Cells. *ACS Appl. Mater. Interfaces.* 6, 17226–17235.

[50] Padinger, F. *et al.* (2003) Effects of Postproduction Treatment on Plastic Solar Cells. *Adv. Funct. Mater.* 13, 85–88.

[51] Schulze, K. *et al.* (2006) Efficient Vacuum-Deposited Organic Solar Cells Based on a New Low-Bandgap Oligothiophene and Fullerene C_{60}. *Adv. Mater.* 18, 2872–2875.

[52] Wynands, D. *et al.* (2006) Correlation between morphology and performance of low bandgap oligothiophene:C60 mixed heterojunctions in organic solar cells. *J. Appl. Phys.* 106, 054509.

[53] Casado, J. *et al.* (2004) Spectroscopic and Theoretical Study of the Molecular and Electronic Structures of a Terthiophene-Based Quinodimethane. *ChemPhysChem* 5, 529–539.

[54] Karpe, S. *et al.* (2007) 3D π-Conjugated Oligothiophenes Based on Sterically Twisted Bithiophene Nodes. *Adv. Funct. Mater.* 17, 1163–1171.

[55] Roquet, S. *et al.* (2006) Three-dimensional tetra(oligothienyl)silanes as donor material for organic solar cells. *J. Mater. Chem.* 16, 3040–3045.

[56] Kleymyuk, E. A. *et al.* (2010) 3D quater- and quinquethiophenesilanes as promising electron-donor materials for BHJ photovoltaic cells and photodetectors. *Energy Environ. Sci.* 3, 1941–1948.

[57] Fischer, M. K. R. *et al.* (2009) Core-functionalized dendritic oligothiophenes - Novel donor-acceptor systems. *J. Mater. Chem.* 19, 4784–4795.

[58] Lanzi, M. *et al.* (2008) New photoactive oligo- and poly-alkylthiophenes. *Polymer* 49, 4942–4948.

[59] Liang, Y. *et al.* (2009) Regioregular Oligomer and Polymer Containing Thieno[3,4-b]thiophene Moiety for Efficient Organic Solar Cells. *Macromolecules* 42, 1091–1098.

[60] Liu, Y. *et al.* (2009) Synthesis and properties of acceptor–donor–acceptor molecules based on oligothiophenes with tunable and low band gap. *Tetrahedron* 65, 5209–5215.

[61] Yin, B. *et al.* (2010) A Solution-Processable Star-Shaped Molecule for High-Performance Organic Solar Cells. *Appl. Phys. Lett.* 97, 023303.

[62] Levichkova, M. *et al.* (2011) Band gap engineering in blended organic semiconductor films based on dielectric interactions. *Org. Electron.* 12, 2243–2252.

[63] Fitzner, R *et al.* (2011) Dicyanovinyl–Substituted Oligothiophenes: Structure-Property Relationships and Application in Vacuum-Processed Small Molecule Organic Solar Cells. *Adv. Funct. Mater.* 21, 897–910.

[64] Fitzner R. *et al.* (2012) Interrelation between Crystal Packing and Small-Molecule Organic Solar Cell Performance. *Adv. Mater.* 24, 675–680.

[65] Fitzner, R. *et al.* (2012) Correlation of π-Conjugated Oligomer Structure with Film Morphology and Organic Solar Cell Performance. *J. Am. Chem. Soc.* 134, 11064−11067.

[66] Haid, S. *et al.* (2011) Dicyanovinylene-Substituted Selenophene–Thiophene Co-oligomers for Small-Molecule Organic Solar Cells. *Chem. Mater.* 23, 4435–4444.

[67] Takimiya, K. *et al.* (2011) Thienoacene-Based Organic Semiconductors. *Adv. Mater.* 23, 4347–4370.

[68] Mishra, A. *et al.* (2014) A–D–A-type S,N-Heteropentacenes: Next-Generation Molecular Donor Materials for Efficient Vacuum‑Processed Organic Solar Cells. *Adv. Mater.* 25, 7217–7223.

[69] Kast, H. *et al.* (2015) Acceptor-Substituted S,N-Heteropentacenes of Different Conjugation Length: Structure–Property Relationships and Solar Cell Performance. *Adv. Funct. Mater.* 25, 3414–3424.

[70] Weidelener, M. *et al.* (2013) Dithienopyrrole-based oligothiophenes for solution-processed organic solar cells. *Chem. Commun.* 49, 10865–10867.

[71] Wessendorf, C. D. *et al.* (2014) Efficiency Improvement of Solution-Processed Dithienopyrrole-Based A-D-A Oligothiophene Bulk-Heterojunction Solar Cells by Solvent Vapor Annealing. *Adv. Energy Mater.* 4, 1400266.

[72] Zhou, J. *et al.* (2011) A Planar Small Molecule with Dithienosilole Core for High Efficiency Solution-Processed Organic Photovoltaic Cells. *Chem. Mater.* 23, 4666–4668.

[73] Ni, W. *et al.* (2015) Dithienosilole-Based Small-Molecule Organic Solar Cells with an Efficiency over 8%: Investigation of the Relationship between the Molecular Structure and Photovoltaic Performance. *Chem. Mater.* 27, 6077−6084.

[74] Cnops, K. *et al.* (2014) 8.4% efficient fullerene-free organic solar cells exploiting long-range exciton energy transfer. *Nat. Commun.* 5:3406.

[75] Hu, H. *et al.* (2015) Terthiophene-Based D–A Polymer with an Asymmetric Arrangement of Alkyl Chains That Enables Efficient Polymer Solar Cells. *J. Am. Chem. Soc.* 137, 14149−14157.

[76] Liu, Y. *et al.* (2014) Aggregation and morphology control enables multiple cases of high-efficiency polymer solar cells. *Nat. Commun.* 5:5293.

[77] Demeter,D. *et al.* (2011) Manipulation of the Open-Circuit Voltage of Organic Solar Cells by Desymmetrization of the Structure of Acceptor–Donor–Acceptor Molecules. *Adv. Funct. Mater.* 21, 4379–4387.

[78] Liu, Y. *et al.* (2011) Spin-Coated Small Molecules for High Performance Solar Cells. *Adv. Energy Mater.* 1, 771–775.

[79] He, G. *et al.* (2014) Impact of fluorinated end groups on the properties of acceptor–donor–acceptor type oligothiophenes for solution-processed photovoltaic cells. *J. Mater. Chem. C* 2, 1337–1345.

[80] Xue, D. *et al.* (2006) Surface Segregation of Fluorinated Moieties on Random Copolymer Films Controlled by Random-Coil Conformation of Polymer Chains in Solution. *Langmuir* 25, 2248–2257.

[81] Li, Z. *et al.* (2012) Solution Processable Rhodanine-Based Small Molecule Organic Photovoltaic Cells with a Power Conversion Efficiency of 6.1%. *Adv. Energy Mater.* 2, 74–77.

[82] Chen, H. *et al.* (2019) Approaching 16% Efficiency in All-Small-Molecule Organic Solar Cells Based on Ternary Strategy with a Highly Crystalline Acceptor. *Joule* 3, 3034–3047.

[83] Xu, T. *et al.* (2021) 15.8% efficiency binary all-small-molecule organic solar cells enabled by a selenophene substituted sematic liquid crystalline donor *Energy Environ. Sci.* 14, 5366–5376.

[84] Tang, H. *et al.* (2020) Benzodithiophene-Based Small-Molecule Donors for Next-Generation All-Small-Molecule Organic Photovoltaics. *Matter* 3, 1403–1432.

[85] He, G. *et al.* (2012) Impact of dye end groups on acceptor–donor–acceptor type molecules for solution-processed photovoltaic cells. *J. Mater. Chem.* 22, 9173–9180.

[86] He, G. *et al.* (2013) Efficient small molecule bulk heterojunction solar cells with high fill factors via introduction of π-stacking moieties as end group. *J. Mater. Chem. A*, 1, 1801–1809.

[87] Long, G. *et al.* (2013) Investigation of Quinquethiophene Derivatives with Different End Groups for High Open Circuit Voltage Solar Cells. *Adv. Energy Mater.* 3, 639–646.

[88] Zhang, Q. *et al.* (2015) Small-molecule solar cells with efficiency over 9%. *Nat. Photon.* 9, 35–41.

[89] Kan, B. *et al.* (2015) A series of simple oligomer-like small molecules based on oligothiophenes for solution-processed solar cells with high efficiency. *J. Am. Chem. Soc.* 137, 3886–3893.

[90] Yan, C. *et al.* (2018) Non-fullerene acceptors for organic solar cells. *Nat. Rev. Mater.* 3, 18003;

[91] Hou, J. *et al.* (2018) Organic solar cells based on non-fullerene acceptors. *Nat. Mater.* 17, 119–128.

[92] Liu, H. *et al.* (2021) Emerging Chemistry in Enhancing the Chemical and Photochemical Stabilities of Fused-Ring Electron Acceptors in Organic Solar Cells. *Adv. Funct. Mater.* 31, 2106735.

[93] Mishra, A. *et al.* (2016) High performance A–D–A oligothiophene-based organic solar cells employing two-step annealing and solution-processable copper thiocyanate (CuSCN) as an interfacial hole transporting layer. *J. Mater. Chem. A* 4, 17344–17353.

[94] Reichenbächer, K. *et al.* (2005) Fluorine in crystal engineering—"the little atom that could". *Chem. Soc. Rev.* 34, 22–30.

[95] Zhang, Q. *et al*. (2017) The Curious Case of Fluorination of Conjugated Polymers for Solar Cells. *Acc. Chem. Res.* 50, 2401–2409.

[96] Zhang, Y. *et al*. (2018) Fluorination vs. chlorination: a case study on high performance organic photovoltaic materials. *Sci. China Chem.* 61, 1328–1337.

[97] Kan, B. *et al*. (2016) Oligothiophene-based small molecules with 3,3'-difluoro-2,2'-bithiophene central unit for solution-processed organic solar cells. *Org. Electron.* 38, 172–179.

[98] Wang, Z. *et al*. (2016) Solution-Processable Small Molecules for High-Performance Organic Solar Cells with Rigidly Fluorinated 2,2'-Bithiophene Central Cores. *ACS Appl. Mater. Interfaces* 8, 11639–11648.

[99] Liang, N. *et al*. (2017) Triperylene Hexaimides Based All-Small-Molecule Solar Cells with an Efficiency over 6% and Open Circuit Voltage of 1.04 V. *Adv. Energy Mater.* 7, 1601664.

[100] Wang, Y. *et al*. (2018) All-Small-Molecule Organic Solar Cells Based on Pentathiophene Donor and Alkylated Indacenodithiophene-Based Acceptors with Efficiency over 8%. *ACS Appl. Energy Mater.* 1, 2150–2156.

[101] Wang, Y. *et al*. (2018) High-Performance All-Small-Molecule Solar Cells Based on a New Type of Small Molecule Acceptors with Chlorinated End Groups. *Adv. Energy Mater.* 8, 1802021.

[102] Yao, H. F. *et al*. (2016) Molecular Design of Benzodithiophene-Based Organic Photovoltaic Materials. *Chem. Rev.* 116, 7397–7457.

[103] McDearmon, B. *et al*. (2018) Organic electronics by design: the power of minor atomic and structural changes. *J. Mater. Chem. C* 6, 3564–3572.

[104] Sun, K. *et al*. (2015) A molecular nematic liquid crystalline material for high-performance organic photovoltaics. *Nat. Commun.* 6:6013.

[105] Qiu, B. *et al*. (2017) All-Small-Molecule Nonfullerene Organic Solar Cells with High Fill Factor and High Efficiency over 10%. *Chem. Mater.* 29, 7543−7553.

[106] Yang, L. *et al*. (2018) Modulating Molecular Orientation Enables Efficient Nonfullerene Small-Molecule Organic Solar Cells. *Chem. Mater.* 30, 2129−2134.

[107] Qin, J. *et al*. (2020) 15.3% efficiency all-small-molecule organic solar cells enabled by symmetric phenyl substitution. *Sci. China Mater.* 63, 1142–1150.

[108] Hu, D. *et al*. (2020) 15.34% efficiency all-small-molecule organic solar cells with an improved fill factor enabled by a fullerene additive. *Energy Environ. Sci.* 13, 2134–2141.

[109] Xu, T. *et al*. (2021) 15.8% efficiency binary all-small-molecule organic solar cells enabled by a selenophene substituted sematic liquid crystalline donor. *Energy Environ. Sci.* 14, 5366–5376.

[110] Babics, M. *et al*. (2019) Negligible Energy Loss During Charge Generation in Small-Molecule/Fullerene Bulk-Heterojunction Solar Cells Leads to Open-Circuit Voltage over 1.10 V. *ACS Appl. Energy Mater.* 2, 2717−2722.

[111] Duan, T. *et al*. (2020) Difluorinated Oligothiophenes for High-Efficiency All-Small-Molecule Organic Solar Cells: Positional Isomeric Effect of Fluorine Substitution on Performance Variations. *Sol. RRL* 4, 1900472.

[112] Xu, T. *et al*. (2020) Fluorinated oligothiophene donors for high-performance nonfullerene small-molecule organic solar cells. *Sustainable Energy Fuels*, 4, 2680–2685.

[113] Duan, T. *et al*. (2020) Simple organic donors based on halogenated oligothiophenes for all small molecule solar cells with efficiency over 11%. *J. Mater. Chem. A*, 8, 5843–5847.

[114] Duan, T. *et al*. (2022) Simple thiazole-centered oligothiophene donor enables 15.4% efficiency all small molecule organic solar cells. *J. Mater. Chem. A* 2022, 10, 3009–3017.

[115] Shi, Y. *et al*. (2021) Optimizing the Charge Carrier and Light Management of Nonfullerene Acceptors for Efficient Organic Solar Cells with Small Nonradiative Energy Losses. *Sol. RRL* 5, 2100008.

[116] Deng, D. *et al*. (2016) Fluorination-enabled optimal morphology leads to over 11% efficiency for inverted small-molecule organic solar cells. *Nat. Commun.* 7:13740.

[117] Zhang, L. *et al*. (2022) High Miscibility Compatible with Ordered Molecular Packing Enables an Excellent Efficiency of 16.2% in All-Small-Molecule Organic Solar Cells. *Adv. Mater.* 2106316.

[118] Camaioni, N. *et al*. (2004) Oligothiophene-S,S-dioxides as a class of electron-acceptor materials for organic photovoltaics. *Appl. Phys. Lett.* 84, 1901.

[119] Ridolfi, G. *et al*. (2005) All-thiophene donor–acceptor blends: photophysics, morphology and photoresponse. *J. Mater. Chem.* 15, 895–901.

[120] Camaioni,N. *et al*. (2005) Branched thiophene-based oligomers as electron acceptors for organic photovoltaics. *J. Mater. Chem.* 15, 2220–2225.

[121] Uhrich, C. *et al*. (2007) Organic Thin-Film Photovoltaic Cells Based on Oligothiophenes with Reduced Bandgap. *Adv. Funct. Mater.* 17, 2991–2999.

[122] Wang, Y. *et al*. (2017) All-Small-Molecule Organic Solar Cells Based on Pentathiophene Donor and Alkylated Indacenodithiophene-Based Acceptors with Efficiency over 8%. *Sol. RRL* 2, 1700179.

[123] Duan, T. *et al*. (2018) F-Substituted oligothiophenes serve as nonfullerene acceptors in polymer solar cells with open-circuit voltages >1 V. *J. Mater. Chem. A* 6, 9368–9372.

[124] Lee, T. *et al.* (2019) Simple Bithiophene–Rhodanine-Based Small Molecule Acceptor for Use in Additive-Free Nonfullerene OPVs with Low Energy Loss of 0.51 eV. *Adv. Energy Mater.* 9, 1804021.

[125] Chen, Y.-N. *et al.* (2020) A Fully Non-fused Ring Acceptor with Planar Backbone and Near-IR Absorption for High Performance Polymer Solar Cells. *Angew. Chem. Int. Ed.* 59, 22714–22720.

[126] Ma, L. *et al.* (2021) Completely non-fused electron acceptor with 3D-interpenetrated crystalline structure enables efficient and stable organic solar cell. *Nat. Commun.* 12:5093.